Inorganic Chemistry

Communication

pubs.acs.org/IC

Zeolitic Metal–Organic Frameworks Based on Amino Acid

E Yang,[†,‡] Lin Wang,[†,‡] Fei Wang,*[,†] Qipu Lin,[†] Yao Kang,[†] and Jian Zhang*[,†]

[†]State Key Laboratory of Structural Chemistry, Fujian Institute of Research on the Structure of Matter, The Chinese Academy of Sciences, Fuzhou, Fujian 350002, P. R. China

[‡]College of Materials Science and Engineering, Fujian Normal University, Fuzhou, Fujian 350007, P. R. China

Supporting Information

ABSTRACT: Two enantiomorphic metal–organic frameworks with zeotype SOD topology have been successfully synthesized from enantiopure L-alanine and D-alanine, respectively, which demonstrates the feasibility of fabricating MOFs that integrate the 4-connected zeotype topologies and homochiral nature by the employment of enantiopure amino acids.

Metal–organic frameworks (MOFs) with well-defined pore structures and promising multifunctionalities are currently of great interest owing to their specific applications in gas storage, separation, and catalysis.[1,2] Among numerous MOFs with diverse structural features, zeolitic MOFs (ZMOFs) with 4-connected zeotype topologies, including zeolitic imidazolate frameworks (ZIFs) and boron imidazolate frameworks (BIFs), continues to attract increasing attention.[3,4] However, homochiral ZMOFs that integrate the zeotype topologies and homochiral nature, to the best of our knowledge, remain highly challenging and rarely known to date.

Great promise in the applications related to heterogeneous asymmetric catalysis and enantioselective separation has stimulated extensive research on homochiral MOFs.[5,6] The most reliable approach to prepare homochiral MOFs is to select an enantiopure ligand as the primary linker to impart homochirality to the frameworks. So far, although tremendous effort has been devoted to the design and synthesis of novel MOFs based on optically pure amino acids and their derivatives, none of them have zeotype structures.[7]

In this work, we first report here two enantiomorphic ZMOFs based on an enantiopure alanine ligand, which show zeotype SOD topology. We choose a pair of enantiopure amino acids (D-alanine and L-alanine) as linkers and highly coordinated Ni(II) as a metal center to probe the feasibility of fabricating homochiral MOFs with 4-connected zeotype topologies. Two enantiomorphic homochiral frameworks, Ni(D-ala)$_2$ (**1D**, D-alaH = D-alanine) and Ni(L-ala)$_2$ (**1L**, L-alaH = L-alanine) with the same formula $NiC_6H_{12}N_2O_4$, are successfully synthesized and structurally characterized.[8,9]

Single crystal X-ray diffraction analysis reveals that **1L** and **1D** are enantiomers of each other and present similar structures. Hence, only the structure of **1D** is discussed here in detail. Blue prism crystal of **1D** crystallizes in the cubic system with chiral space groups *I*23, and the Flack parameter of 0.01(4) demonstrates the homochiral nature of the single crystal. The asymmetric unit of **1D** consist of a half Ni(II) ion and one D-alanine anion. Each central Ni(II) ion is coordinated by two carboxylate oxygen atoms and two nitrogen atoms from two separated D-alanine anions, two carboxylate oxygen atoms from other two separated D-alanine anions, giving rise to a [NiO_4N_2] octahedral geometry (Figure 1a). The bond lengths

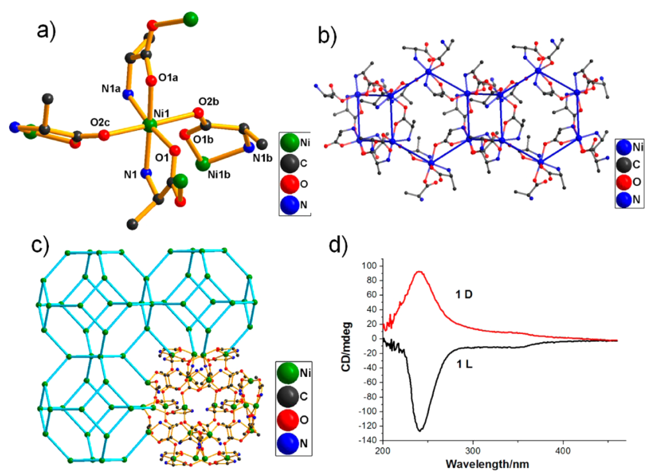

Figure 1. (a) The coordination environment in **1D** with hydrogen atoms omitted for clarity. Symmetry codes: (a) $-x + 2, y, -z + 1$; (b) $z + 1/2, -x + 3/2, -y + 3/2$; (c) $-z + 3/2, -x + 3/2, y - 1/2$. (b) Partial plot of the network in **1D**. (c) The SOD-type framework structure of **1D**. (d) The solid-state CD spectra of bulk samples of **1L** and **1D**.

of Ni1–O1, Ni1–O2, and Ni1–N1 are 2.014(3), 2.134(3), and 2.072(3)Å, respectively. Each six coordinated Ni(II) ion connects four neighboring Ni(II) ions through four D-alanine anions into a three-dimensional open framework with a Ni···Ni distance of 4.996(7) Å.

Notably, a remarkable structural feature in **1D** is the presence of a three-dimensional 4-connected SOD network. In the structure of **1D**, the D-alanine anion chelating to the Ni(II) metal center via one nitrogen atom and one carboxylate oxygen atom, the remaining one carboxylate oxygen atom connects another Ni(II) metal center. Hence, the D-alanine anion acts as a μ_2-bridging ligand. Owing to the unique chelating mode of the D-alanine anion, consuming two bonding sites of a 6-coordinate Ni(II) center, the 6-coordinate Ni(II) center can be successful reduced as a 4-connected node. As a result, the whole framework can be topologically represented as a uninodal 4-

Received: June 30, 2014
Published: September 5, 2014

connected zeotype SOD topology by considering the D-alanine anion as simple bridge linker (Figure 1b,c).

The solid-state circular dichroism (CD) measurements performed on bulk samples of **1L** and **1D** in a pressed dry KCl disk further verify the fact of the homochiral crystallization between Ni^{2+} cations and enantiopure amino acids (Figure 1d). The CD spectrum for the bulk sample of **1L** exhibits a negative CD signal at 241 nm, while a positive CD signal appears at 240 nm for the bulk sample **1D**. The CD spectra for the bulk samples of **1L** and **1D** show an almost mirror image of each other, demonstrating that compounds **1L** and **1D** are a pair of enantiomers. The outcomes from the CD spectra are consistent with the results obtained by single-crystal structure refinements. It is also demonstrated that chirality transfer from optically pure ligands happened in the generation of a homochiral crystal.[7]

The powder X-ray diffraction (PXRD) patterns of compounds **1D** and **1L** are in good agreement with the simulated ones on the basis of the single-crystal structure, respectively, confirming the phase purity of these bulk products (Figure S1). To investigate their thermal behaviors, thermogravimetric (TG) analysis studies were carried out on preweighed samples under a N_2 atmosphere with a heating rate of 10 °C min^{-1} (Figure S2). The TG curve of **1D** is almost the same as that of **1L**. The TG plot of **1D** shows an obvious plateau between 30 and 300 °C, indicating no obvious weight loss up to 300 °C, confirming no guest molecule reside in the framework of **1D**. After 300 °C, the ligands onset release and the framework decomposition started.

Since **1L** and **1D** are enantiomers of each other and manifest the similar structure, we only choose **1L** to investigate the magnetic properties. The temperature dependence of magnetic susceptibility for **1L** is investigated in the range 2 K to room temperature under a 1 kOe applied field (Figure 2). The

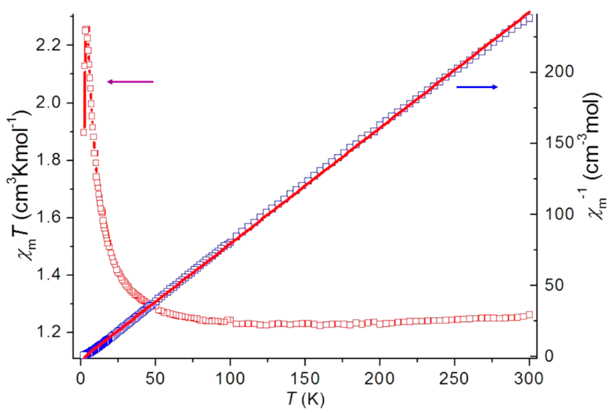

Figure 2. Temperature dependence of $\chi_m T$ and χ_m^{-1} for compound **1L** in an applied field of 1 kOe.

observed $\chi_m T$ value of 1.26 cm^3 K mol^{-1} at room temperature is close to the spin only value of uncoupled $S = 1$ Ni^{2+} ion with g of ca. 2.24 and remains nearly constant down to about 60 K. Upon further cooling, $\chi_m T$ continuously increases to reach a maximum value of 2.25 cm^3 K mol^{-1} at 3.5 K, indicating dominant ferromagnetic exchange,[10] and then subsequently goes down to 1.90 cm^3 K mol^{-1} at 2 K. The decrease in low temperature zone might be due to the effect of saturation and/or zero-field splitting of the anisotropic Ni^{2+} ion. In view of the 3D periodic nature of **1L**, these features suggest the onset of long-range ferromagnetic ordering, consistent with the frequency-independent rises of both in-phase (χ_m') and out-of-phase (χ_m'') zero-field ac magnetic susceptibility (Hac = 3 Oe; Figure S3 and S4). But no peak was observed in ac magnetization, coupled with no bifurcation in the zero-field-cooled (zfc) and field-cooled (fc) susceptibility, indicating the critical temperature Tc of being <2 K (beyond the detection limit).

A detailed quantitative analysis of the susceptibility data for 3D extended Ni^{2+} complexes is considerably complicated also by the fact of single-ion anisotropic effects etc. In the case of **1L**, the thermo-magnetic data in nearly the whole range can be fitted to the Curie−Weiss expression with a Weiss constant θ = 2.14 K, matching the ferromagnetic interaction between Ni^{2+} ions in the L-alanine bridged 3D matrix. The field dependence of the magnetization (M) in the field range from −8 to +8 T was measured at 2 K (Figure S5). The fast-saturated variations on the isothermal magnetization (M) vs the applied field (H) curve further confirm the dominant ferromagnetic coupling for Ni-based **1L** (Figure S6). The saturation value (M_s) of 1.88 $N\beta$ for **1L** is consistent with the moment of one Ni^{2+} ion. Yet, negligible hysteresis loop was observed, indicating that **1L** can be referred to as very soft ferromagnets.

In summary, two enantiomorphic MOFs with zeotype SOD topology have been successfully synthesized from enantiopure L-alanine and D-alanine, respectively. This work demonstrates the feasibility of fabricating ZMOFs that integrate the 4-connected zeotype topologies and homochiral nature by the employment of enantiopure amino acids.

■ ASSOCIATED CONTENT

Supporting Information

TGA curve and powder XRD patterns. This material is available free of charge via the Internet at http://pubs.acs.org.

■ AUTHOR INFORMATION

Corresponding Authors

*E-mail: wangfei04@fjirsm.ac.cn.

*E-mail: zhj@fjirsm.ac.cn.

Notes

The authors declare no competing financial interest.

■ ACKNOWLEDGMENTS

We thank the support of this work by 973 program (2012CB821705 and 2011CB932504), NSFC (21103189, 21173224, 21221001), and CAS (XDA07070200).

■ REFERENCES

(1) (a) Zhang, J.-P.; Zhang, Y.-B.; Lin, J.-B.; Chen, X.-M. *Chem. Rev.* **2012**, *112*, 1001−1033. (b) Zhao, X.; Bu, X.; Wu, T.; Zheng, S.-T.; Wang, L.; Feng, P. *Nat. Commun.* **2013**, *4*, 2344 DOI: 10.1038/ncomms3344. (c) Zhang, H.-X.; Liu, M.; Bu, X.; Zhang, J. *Sci. Rep.* **2014**, *4*, 3923 DOI: 10.1038/srep03923.

(2) (a) Ma, L.; Abney, C.; Lin, W. *Chem. Soc. Rev.* **2009**, *38*, 1248−1256. (b) Zhai, Q.; Lin, Q.; Wu, T.; Wang, L.; Zheng, S.; Bu, X.; Feng, P. *Chem. Mater.* **2012**, *24*, 2624−2626. (c) Kong, G.-Q.; Ou, S.; Zou, C.; Wu, C.-D. *J. Am. Chem. Soc.* **2012**, *134*, 19851−19857. (d) He, Y.; Zhou, W.; Yildirim, T.; Chen, B. *Energy Environ. Sci.* **2013**, *6*, 2735−2744. (e) Zhou, H.-C.; Long, J. R.; Yaghi, O. M. *Chem. Rev.* **2012**, *112*, 673−674. (f) Darensbourg, D. J.; Chung, W.-C.; Wang, K.; Zhou, H.-C. *ACS Catal.* **2014**, *4*, 1511−1515. (g) Lu, G.; Li, S.; Guo, Z.; Farha, O. K.; Hauser, B. G.; Qi, X.; Wang, Y.; Wang, X.; Han, S.; Liu, X.; DuChene, J. S.; Zhang, H.; Zhang, Q.; Chen, X.; Ma, J.; Joachim Loo, S. C.; Wei, W. D.; Yang, Y.; Hupp, J. T.; Huo, F. *Nat. Chem.* **2012**, *4*, 310−316. (h) Gu, Z.-Y.; Park, J.; Raiff, A.; Wei, Z.; Zhou, H.-C. *Chem.*

Catal. Chem. **2013**, *6*, 67–75. (i) Gao, J.; Bai, L.; Zhang, Q.; Li, Y.; Rakesh, G.; Lee, J. M.; Yang, Y.; Zhang, Q. *Dalton Trans.* **2014**, *43*, 2559–2565. (j) Gao, J.; Miao, J.; Li, P.-Z.; Teng, W. Y.; Yang, L.; Zhao, Y.; Liu, B.; Zhang, Q. *Chem. Comm.* **2014**, *50*, 3786–3788. (k) Lu, H.-S.; Bai, L.; Xiong, W.-W.; Li, P.; Ding, J.; Zhang, G.; Wu, T.; Zhao, Y.; Lee, J.; Yang, Y.; Geng, B.; Zhang, Q. *Inorg. Chem.* **2014**, DOI: 10.1021/ic5011133.

(3) (a) Liu, Y. L.; Kravtsov, V. C.; Larsen, R.; Eddaoudi, M. *Chem. Commun.* **2006**, 1488–1490. (b) Tian, Y.; Yao, S.; Gu, D.; Cui, K.; Guo, D.; Zhang, G.; Chen, Z.; Zhao, D. *Chem.—Eur. J.* **2010**, *16*, 1137–1141. (c) Huang, X.-C.; Lin, Y.-Y.; Zhang, J. P.; Chen, X.-M. *Angew. Chem., Int. Ed.* **2006**, *45*, 1557–1559. (d) Phan, A.; Doonan, C.; Uribe-Romo, F. J.; Knobler, C. B.; O'keeffe, M.; Yaghi, O. M. *Acc. Chem. Res.* **2009**, *43*, 58–67. (e) Wang, S.; Zhao, T.; Li, G.; Wojtas, L.; Huo, Q.; Eddaoudi, M.; Liu, Y. *J. Am. Chem. Soc.* **2010**, *132*, 18038–18041.

(4) (a) Wu, T.; Zhang, J.; Zhou, C.; Wang, L.; Bu, X.; Feng, P. *J. Am. Chem. Soc.* **2009**, *131*, 6111–6113. (b) Wang, F.; Shu, Y.-B.; Bu, X.; Zhang, J. *Chem.—Eur. J.* **2012**, *18*, 11876–11879. (c) Nouar, F.; Eckert, J.; Eubank, J. F.; Forster, P.; Eddaoudi, M. *J. Am. Chem. Soc.* **2009**, *131*, 2864–2870. (d) Fang, Q.; Zhu, G.; Xue, M.; Sun, J.; Wei, Y.; Qiu, S.; Xu, R. *Angew. Chem., Int. Ed.* **2005**, *44*, 3845–3848.

(5) (a) Seo, J. S.; Whang, D.; Lee, H.; Jun, S. I.; Oh, J.; Jeon, Y. J.; Kim, K. *Nature* **2000**, *404*, 982–986. (b) Ma, L.; Abney, C.; Lin, W. *Chem. Soc. Rev.* **2009**, *38*, 1248–1256. (c) Morris, R. E.; Bu, X. *Nat. Chem.* **2010**, *2*, 353–361.

(6) (a) Liu, Y.; Xuan, W.; Cui, Y. *Adv. Mater.* **2010**, *22*, 4112–4135. (b) Xiong, R.-G.; You, X.-Z.; Abrahams, B. F.; Xue, Z.; Che, C.-M. *Angew. Chem., Int. Ed.* **2001**, *40*, 4422–4425.

(7) (a) Vaidhyanathan, R.; Bradshaw, D.; Rebilly, J.-N.; Barrio, J. P.; Gould, J. A.; Berry, N. G.; Rosseinsky, M. J. *Angew. Chem., Int. Ed.* **2006**, *45*, 6495–6499. (b) Appelhans, L. N.; Kosa, M.; Venkataramana, R.; Simoncic, P.; Navrotsky, A.; Parrinello, M.; Cheetham, A. K. *J. Am. Chem. Soc.* **2009**, *131*, 15375–15386. (c) Dybtsev, D. N.; Nuzhdin, A. L.; Chun, H.; Bryliakov, K. P.; Talsi, E. P.; Fedin, V. P.; Kim, K. *Angew. Chem., Int. Ed.* **2006**, *45*, 916–920. (d) Tan, Y. X.; He, Y. P.; Zhang, J. *Inorg. Chem.* **2011**, *50*, 11527–11531.

(8) Synthesis of Ni(D-ala)$_2$ (**1D**): the mixture of $Ni(NO_3)_2 \cdot 6H_2O$ (0.7509 g), D-alanine (0.2797g), $KB(im)_4$ (0.5495g), and N,N-dimethylformamide (10 mL) was sealed in a 23 mL Teflon-lined autoclave and kept at 120 °C for 6 days. After cooling to room-temperature, the blue crystals were obtained in pure phase (yield: 35%). Synthesis of Ni(L-ala)$_2$ (**1L**): This phase was synthesized in an analogous procedure to **1D** except that L-alanine was used in place of D-alanine. Elemental analysis for $NiC_6H_{12}N_2O_4$ Calcd.: C, 30.65; H, 5.15; N, 11.92. Found, 1L: C, 30.88; H, 5.58; N, 12.62; 1D, C: 31.27, H: 5.86, N: 11.74.

(9) Crystal data for **1D**: $C_6H_{12}N_2O_4Ni$, M = 234.89, Cubic, $a = b = c$ = 14.1165(2) Å, V = 2813.07(7) Å^3, T = 293(2) K, space group $I23$, Z = 12, 1243 reflections measured, 855 independent reflections (R_{int} = 0.0210). The final R_1 value was 0.0344 ($I > 2\sigma(I)$). The final $wR(F^2)$ value was 0.0692 ($I > 2\sigma(I)$). The final R_1 value was 0.0449 (all data). The final $wR(F^2)$ value was 0.0776 (all data). The goodness of fit on F^2 was 1.075. The Flack parameter was 0.01(4). CCDC-1002546–1002547.

(10) (a) Guo, S.-Q.; Tian, D.; Zheng, X.; Zhang, H. *CrystEngComm* **2012**, *14*, 3177–3182. (b) Duan, L.-M.; Xie, F.-T.; Chen, X.-Y.; Chen, Y.; Lu, Y.-K.; Cheng, P.; Xu, J.-Q. *Cryst. Growth Des.* **2006**, *5*, 1101–1106.